

Determination of the energy scale of cosmic ray measurements using the Auger Engineering Radio Array

Tim Huege^{ab,*} for the Pierre Auger Collaboration^c

^a*Institute for Astroparticle Physics, Karlsruhe Institute of Technology, P.O. Box 3640, Karlsruhe, Germany*

^b*Astrophysical Institute, Vrije Universiteit Brussel, Pleinlaan 2, 1050 Brussel, Belgium*

^c*Observatorio Pierre Auger, Av. San Martín Norte 304, 5613 Malargüe, Argentina*

Full author list: https://www.auger.org/archive/authors_icrc_2025.html

E-mail: spokespersons@auger.org

The accurate determination of the absolute energy scale in cosmic ray measurements is both a challenging and fundamentally important task. We present how measurements of radio pulses from extensive air showers with the Auger Engineering Radio Array, combined with per-event simulations of radio emission using the CoREAS extension of CORSIKA, allow us to determine the energy scale of cosmic rays between $3 \cdot 10^{17}$ eV and several 10^{18} eV. Our analysis accounts for many factors, each of which is controlled on the 5% level or better. The absolute calibration of the antennas and the entire analog signal chain builds on a Galactic calibration in combination with a detailed understanding of the antenna-gain patterns. Additional key elements include compensation for temperature-dependent signal amplification, continuous detector health monitoring, an active veto for thunderstorm conditions, an unbiased event reconstruction, and per-event atmospheric modeling in the simulations. The analysis benefits from a high-statistics dataset of over 800 measured cosmic ray showers. We describe our analysis method, perform multiple cross-checks, and evaluate systematic uncertainties. We find that absolute energies determined with AERA are 12% higher than those established with the Auger Fluorescence Detector, a result well in agreement within systematic uncertainties and thus a strong independent confirmation of the absolute energy scale of the Pierre Auger Observatory.

*Speaker

1. Introduction

A major challenge in the measurement of ultra-high-energy cosmic rays through air showers is the accurate determination of the absolute energy scale of the measured particles. At the Pierre Auger Observatory, the energy scale is determined with the Fluorescence Detector (FD). This approach avoids relying on simulations suffering from uncertainties in hadronic interaction models. In short, a well-calibrated measurement of the fluorescence light, directly proportional to the energy deposited by the air-shower particles in the atmosphere, is combined with precision atmospheric monitoring to determine the *calorimetric energy* of individual air showers and then use this measurement to cross-calibrate the measurements with the water-Cherenkov detectors of the Surface Detector (SD) [1]. The FD energy scale underlying this work is the one underlying our most recent energy spectrum [2], with the difference that here it is applied to the SD-750 array instead of the SD-1500 array. It reflects minor improvements over the most recent published SD-750 energy spectrum [3].

With the availability of radio antennas in the form of the *Auger Engineering Radio Array* (AERA), consisting of 153 autonomous detector stations covering an area of 17 km^2 and measuring signals in the 30–80 MHz band [4], an independent possibility arises to determine and validate the energy scale of the observatory. Fundamentally, the approach is similar to the one based on the FD, as also the total *radiation energy* emitted by an air shower¹, after applying well-known density corrections, is a calorimetric measurement of the energy in the electromagnetic cascade [5]. A well-calibrated radio detector and knowledge of the expected *radiation energy* for a given *electromagnetic energy*, either from first-principles microscopic Monte-Carlo simulations or from laboratory measurements, can then provide an independent measure of the energy scale of the observatory [6]. In the following, we describe how we establish the energy scale of cosmic-ray measurements from radio signals in the energy range of $3 \cdot 10^{17}$ to several 10^{18} eV with a high-quality data set of air showers measured with AERA and simulated with the CoREAS [7] code.

2. Determination of the energy scale with AERA

The logic of the analysis is shown in Fig. 1. For an air shower measured with the SD, we reconstruct the *shower energy* E_{SD} , the absolute scale of which has previously been established with the FD. This energy, also called *cosmic-ray energy*, estimates the total energy in the air shower, including contributions which are visible neither to the FD nor to radio antennas. The so-called *invisible energy* has previously been determined in a data-driven way as a function of *cosmic-ray energy* [8]. After subtracting the *invisible energy* from the *shower energy*, we have an estimate of the *calorimetric energy*, i.e., the total energy deposited in the atmosphere by the electromagnetic cascade, on the energy scale set by the FD. Using the air-shower geometry and this *calorimetric energy* estimate from the SD, we then set up a CORSIKA [9] simulation of the corresponding air shower, along with radio-emission simulations with the CoREAS [7] extension, such that the resulting simulated shower will have the target *calorimetric energy*.

In a final step, we reconstruct the *radiation energy* measured with AERA [10] for both the measured shower (which is on the *radio energy scale*) as well as for the simulated shower (which is

¹The total energy radiated in the form of radio waves, in the case of AERA in the 30–80 MHz band.

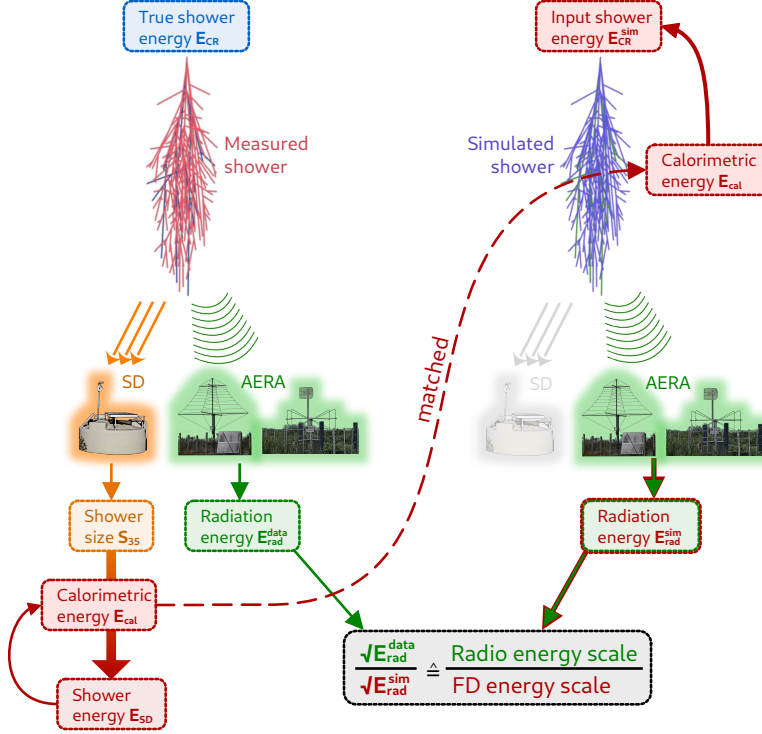


Figure 1: Logic for event-by-event comparison of measured and simulated air showers, determining the agreement between the FD and radio energy scales. Observables depicted in red are on the FD energy scale. The orange and green colors represent SD and radio measurements, respectively.

on the *FD energy scale*, as the input energy for the simulation is based ultimately on the *FD energy scale*). The ratio of the reconstructed *radiation energies* reconstructed from the measurements and simulations then determines the ratio between the *radio energy scale* and the *FD energy scale*.

While the logic of this analysis is seemingly simple, the challenge lies in the fact that systematic uncertainties on all involved detectors and their corresponding event reconstructions need to be understood on a 5% level or better to provide a result with the desired accuracy. In terms of the absolute calibration of AERA, this requires in particular knowledge of the frequency-dependent antenna-gain patterns of the used LPDA and butterfly antennas [4] (known to within 5%) and the absolute calibration of the radio measurements from a comparison of the Galactic radio emission (known at a level of 6%) with the measured radio emission over full local sidereal days [11, 12]. The AERA event reconstruction [10] of the *radiation energy* has previously been demonstrated to be bias-free irrespective of the type of primary particle. The signal processing with the Offline analysis framework [13] is carried out in the exact same way on simulations and data, so that any minor biases possibly arising from analysis steps such as bandpass filtering or signal cleaning affect data and simulations in the same way and thus cancel out in the final ratio.

3. Event selection and simulation production

We begin with a data set of 3,245 air showers measured in the period from 2014 to 2020 with the 750 m array of the SD, passing standard SD quality cuts, having their cores contained within the

geometrical area of the AERA stations capable of accepting an SD trigger, and having reconstructed SD energies of at least $3 \cdot 10^{17}$ eV, thus ensuring full detection efficiency of the SD. Exclusion of confirmed thunderstorm periods [14] or periods with no data on thunderstorm activity reduces the data set to 3,015 air showers. For these 3,015 events, we perform a reconstruction of the *radiation energy* E_{rad} from the data of the AERA stations that are able to receive an external trigger from the SD and were fully functional at the time of measurement. The main criterion that 5 AERA stations had a signal amplitude a factor of $\sqrt{10}$ above the noise-RMS reduces the data set to 1,096 air showers. Requiring some quality cuts on reconstructed uncertainties results in a data set of 902 air showers with a valid E_{rad} reconstruction. Applying further cuts to ensure high data quality as listed in the upper half of Tab. 1 results in a data set of 844 air showers on which the remainder of the analysis builds.

For each of these 844 air showers we prepare one CoREAS simulation each with a proton and an iron primary according to the logic described above. The chosen interaction models are Sybill 2.3d and UrQMD. We note, however, that our result does not depend on the choice of hadronic interaction model as the radio emission is purely sensitive to the electromagnetic cascade of the air shower and we subtract the *invisible energy* of the chosen hadronic interaction model in a self-consistent way. For the simulations, we adopt a per-event atmospheric density and refractivity gradient [15] derived from the Global Data Assimilation System (GDAS). Furthermore, very conservative settings on particle thinning and a fine-grained treatment of multiple scattering (STEPFC parameter of 0.05) [16] ensure absolute signal predictions with the highest-possible accuracy. The simulated radio signals are then fed through a detailed detector simulation with the Offline analysis framework [13], including the addition of measured background noise taken at a given antenna station within 10 minutes of the measured event, before being reconstructed in the exact same way as the data.

As expected, not all simulations pass the E_{rad} reconstruction, since AERA is not fully efficient at the lower end of this energy range. In particular, deep low-energy showers might not illuminate the required 5 AERA stations with sufficient signal strength. The survival probability for iron-induced showers is higher than that of proton showers. The AERA data set will thus no longer be unbiased. As the radio emission is only associated with the *electromagnetic energy*, this is not a critical problem, in a similar way that the chosen hadronic interaction model does not influence the result of the analysis. However, this potential shift towards a heavier mass composition could introduce second-order effects on the mean of the reconstructed SD energies, which we have estimated from simulations to be less than 2.4%, and which we thus account for with a corresponding systematic uncertainty. The same additional quality cuts previously applied to the measured data and listed in Tab. 1 reduce the total number of usable simulations to 537 and 674 for proton- and iron-induced air showers, respectively. The distributions of E_{SD} , arrival azimuth angle and arrival zenith angle for the 844 selected events as well as the surviving simulations for proton and iron primaries are shown in Fig. 2.

We note that during the complete development of the analysis (concerning the choice of cuts, optimization of the event reconstruction, etc.), we applied an unknown, global “blinding factor” to the measured radiation energies, as to not unconsciously influence the result in a “favorable” direction. This blinding factor was only lifted after the analysis was completely defined.

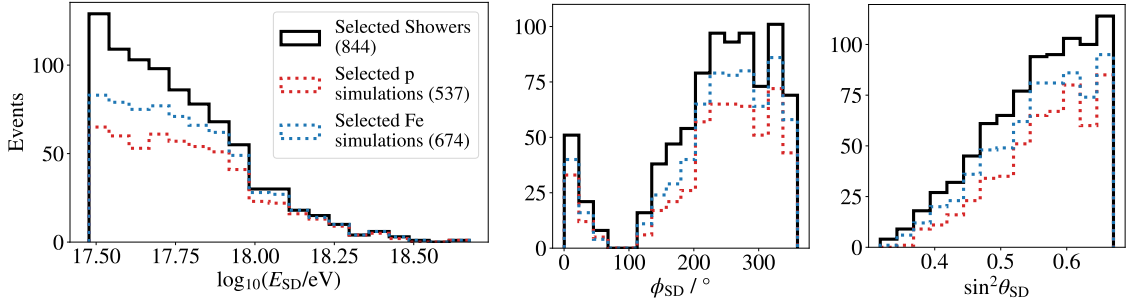


Figure 2: Left: Distribution of the logarithmic SD-reconstructed energies of the quality event set of 844 air showers and the proton and iron simulation sets after reconstruction and quality cuts. Middle and Right: Distributions of the azimuth angle, counter-clockwise from geographic East, and the zenith angle, as reconstructed with the SD for the same data and simulation sets.

Table 1: Quality selection cuts for the event set. Survival fractions relate to the previous selection step. χ^2/ndf refers to the quality of the LDF fit, α is the geomagnetic angle.

| Cut or requirement | N_{events} | Survival fraction |
|---|---------------------|-------------------|
| After SD cuts & base cuts (see text) | 902 | |
| Additional radio cuts on data | | |
| No saturated stations within 500 m | 873 | 96.8% |
| $\chi^2/N_{\text{df}} < 10$ | 854 | 97.8% |
| $\alpha > 20^\circ$ | 844 | 98.8% |
| Radio cuts on simulations | | |
| $N_{\text{stations,signal}} \geq 5$ | 549 / 684 | 65.0% / 81.0% |
| E_{rad} reconstructed | 542 / 678 | 98.7% / 99.1% |
| $\sigma_{E_{\text{rad}}}$ reconstructed | 538 / 677 | 99.3% / 99.9% |
| Radio core reconstructed | 538 / 676 | 100.0% / 99.9% |
| No saturated stations within 500 m | 538 / 676 | 100.0% / 100.0% |
| $\chi^2/\text{ndf} < 10$ | 537 / 676 | 99.8% / 100.0% |
| $\alpha > 20^\circ$ | 537 / 674 | 100.0% / 99.7% |

4. Results on the energy scale

In Fig. 3, we present histograms of the ratios of *radiation energies* for measured and simulated events, once for the proton and once for the iron simulations. The square root of the ratio is taken because the *radiation energy* scales with the square of the *electromagnetic energy* due to the coherent nature of the radio emission. We bin in \log_{10} of the ratios rather than simple ratios, thereby ensuring symmetry between ratios smaller and larger than unity. The linear scale factors resulting from the means of the shown distributions for proton and iron simulations are indicated at the top axes of the diagrams. The two scale factor are compatible within statistical uncertainties – as expected, there is no systematic difference induced by the type of primary particle. Averaging the two mean values and afterwards compensating for the \log_{10} operation yields that

$$\frac{\text{Radio energy scale}}{\text{FD energy scale}} = 1.120^{+0.009}_{-0.008} \text{ (stat)}, \quad (1)$$

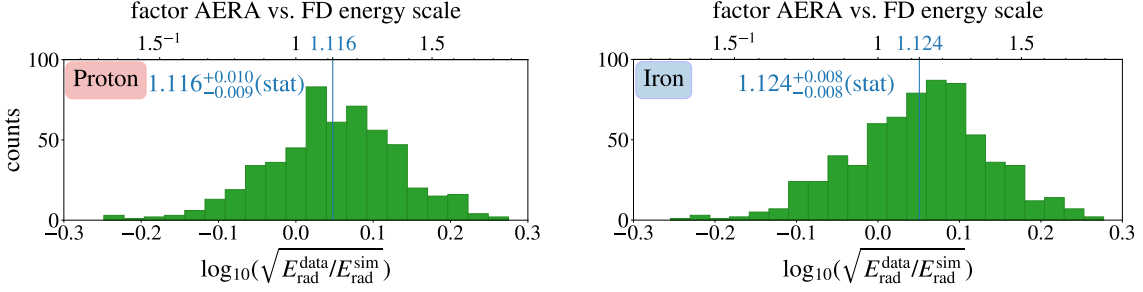


Figure 3: Distribution of the logarithm of the square root ratios of the reconstructed radiation energies for measured events with the two simulation sets. *Left:* result for proton simulations, *Right:* result for iron simulations. The resulting mean scale factors are indicated on the top axes.

where the quoted $\sim 0.8\%$ uncertainty refers to statistical uncertainties only. This result signifies that the energy scale determined from radio data is 12% higher than the FD energy scale. In other words: A 10^{18} eV air shower measured on the FD energy scale has an energy of $1.12 \cdot 10^{18}$ eV on the energy scale determined from radio data.

We have stratified our data in many different ways to check for potential correlations with arrival direction, core position, ambient temperature, year of data taking, number of signal stations and SD-reconstructed shower energy. None of the tests showed any significant correlations. In Fig. 4, we show the \log_{10} of the square root ratios as a function of time (left) and E_{SD} (right). The fact that there is no time-evolution confirms that the radio measurement is not suffering from detector ageing [12]. The fact that the scale factor remains constant over a decade in energy means that there is no slope between the FD and radio energy scales, another important and non-trivial result.

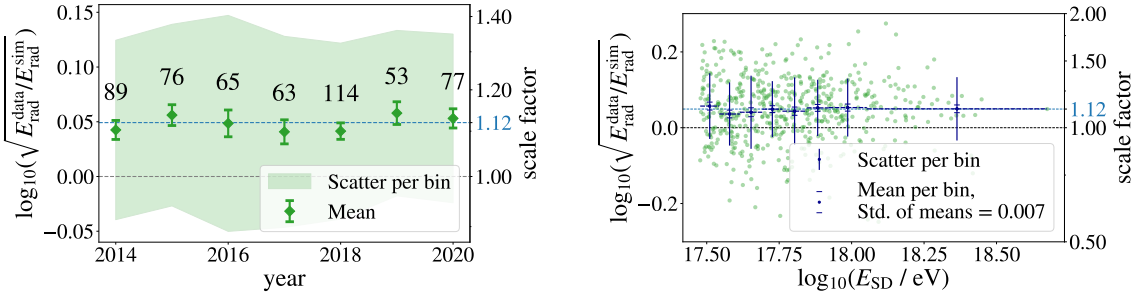


Figure 4: *Left:* Evolution of the mean of the logarithmic square root ratio of radiation energies across the years covered by the event set, for proton simulations. *Right:* Dependence of the mean logarithmic square root ratio of radiation energies on the SD-reconstructed shower energy.

5. Systematic uncertainties

We have performed an in-depth investigation of systematic uncertainties affecting the result, listed in Tab. 2. Of the experimental uncertainties, the most important ones are the accuracy of the Galactic calibration arising from performing the calibration with a total of 7 available sky models, interpreting the spread of the resulting calibration constants as a systematic uncertainty amounting to 6.1%. Uncertainties still remaining in our understanding of the antenna response pattern, in

particular for the butterfly antennas, add an additional 5%. Drone-based calibration campaigns are ongoing and have the potential to lower this uncertainty in the future. The systematic uncertainty resulting from a potential bias of the mass composition towards heavier elements due to inefficiency of AERA in detecting deep showers is conservatively estimated to 2.4%. All other investigated uncertainties are negligible in comparison.

Of the uncertainties related to predicting the absolute strength of the radio emission, the dominant one with 5.1% is the “radio emission yield”, i.e., the relation between the absolute radio-emission strength and the energy in the underlying electromagnetic cascade. This value results from in-depth comparisons of independent implementations of both the simulations of extensive air showers and their associated radio emission with first-principle classical electrodynamics within CORSIKA 7, ZHAireS, CORSIKA 8 [16, 17] and with the “endpoints” and ZHS formalisms [17]. In terms of experimental verification, the only measurement available so far is that of the SLAC T-510 experiment, which showed agreement between measured and simulated signals on the level of 5% with a systematic uncertainty of $\sim 10\%$ [18]. Again, other systematic uncertainties related to the signal prediction are negligible.

If one accepts the spread on the radio-emission between different microscopic simulations as the systematic uncertainty on the “radio emission yield”, the total systematic uncertainty on the energy scale determined from AERA amounts to 10.2%. Taking a more conservative approach based on the SLAC T-510 measurement results in a total systematic uncertainty of 13.4%. The systematic uncertainty of the FD energy scale amounts to 14%. Statistical uncertainties amount to 0.8% and are thus negligible in comparison with systematic uncertainties. Assuming the uncertainties of the FD and AERA-determined energy scales to be uncorrelated and thus summing them in quadrature, for the case of the simulations-based radio-emission yield uncertainty, thus results in

$$\frac{\text{Radio energy scale}}{\text{FD energy scale}} = 1.120 \pm 0.173 \text{ (sys)} {}^{+0.009}_{-0.008} \text{ (stat)}. \quad (2)$$

The energy scales determined from the FD and AERA are thus well in agreement within systematic uncertainties.

6. Conclusions

We have used a high-quality data set of 844 air showers measured with AERA in the energy range from $3 \cdot 10^{17}$ eV to several 10^{18} eV in comparison with simulations of the same air showers using the CoREAS code to independently determine the absolute energy scale of cosmic-ray measurements at the Pierre Auger Observatory using radio signals. Particular care has been taken in crafting an analysis that does not suffer from biases and in which all individual systematic uncertainties are under control at the 5% level. The analysis was developed using a blinded data set to avoid subconscious influence on the analysis and the choice of selection cuts. The end result is that the energy scale determined from AERA is 12% higher than the one from the FD, a constant factor over the investigated energy range and the period from 2014 to 2020. The systematic uncertainty on the energy scale determined from radio data amounts to 10.3% when building on the “radio emission yield” uncertainty estimated from simulations, or 13.4% when relying on the measurement uncertainty reported by the SLAC T-510 experiment. The energy scale derived

Table 2: Summary of uncertainties on the radio energy scale.

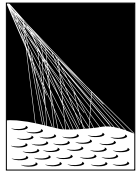
| Source of uncertainty | Size |
|--|---|
| Experimental uncertainties | 8.8 % |
| Galactic calibration | 6.1 % |
| Antenna response pattern | 5 % |
| LDF model | 0.5 % |
| Atmosphere | <1.25 % |
| Ground conditions | <1.8 % |
| Quiet sun | 0.5 % |
| Simulation primary bias | 1.9 % |
| Mass composition bias w.r.t. Auger mix | 2.4 % |
| Theoretical uncertainties | 5.1 % / ~10.1 % |
| Radio emission yield | 5.0 % / ~10 % |
| Choice of hadronic interaction model | 0.13 % |
| Thinning | <0.15 % |
| Energy thresholds of shower particles | <0.5 % |
| Stat. unc. of energy scale comparison | 0.8 % |
| Total absolute scale uncertainty | Stat.: 0.8 % Syst.: 10.2 % / ~13.4 % |

from AERA is well in agreement with the Auger energy scale determined from measurements with the Fluorescence Detector, a strong and independent confirmation of the FD energy scale within systematic uncertainties. In the future, we will use the Auger Radio Detector covering the full 3,000 km² of the observatory to also independently determine the energy scale at the highest energies from radio measurements.

References

- [1] PIERRE AUGER collaboration, *PoS ICRC2019* (2020) 231.
- [2] PIERRE AUGER collaboration, arXiv:2506.11688.
- [3] PIERRE AUGER collaboration, *Eur. Phys. J. C* **81** (2021) 966 [2109.13400].
- [4] PIERRE AUGER collaboration, *JINST* **7** (2012) P10011 [1209.3840].
- [5] C. Glaser, M. Erdmann, J.R. Hörandel, T. Huege and J. Schulz, *JCAP* **09** (2016) 024 [1606.01641].
- [6] PIERRE AUGER collaboration, *Phys. Rev. Lett.* **116** (2016) 241101 [1605.02564].
- [7] T. Huege, M. Ludwig and C.W. James, *AIP Conf. Proc.* **1535** (2013) 128 [1301.2132].
- [8] PIERRE AUGER collaboration, *Phys. Rev. D* **100** (2019) 082003 [1901.08040].
- [9] D. Heck, J. Knapp, J.N. Capdevielle, G. Schatz and T. Thouw, FZKA Report 6019 (1998), DOI.
- [10] PIERRE AUGER collaboration, *Phys. Rev. D* **93** (2016) 122005 [1508.04267].
- [11] M. Büskens, T. Fodran and T. Huege, *Astron. Astrophys.* **679** (2023) A50 [2211.03086].
- [12] PIERRE AUGER collaboration, *PoS ARENA2024* (2024) 030 [2410.13591].
- [13] PIERRE AUGER collaboration, *Nucl. Instrum. Meth. A* **635** (2011) 92 [1101.4473].
- [14] M. Gottowik, Ph.D. thesis, University of Wuppertal, 2021.
- [15] P. Mitra et al., *Astropart. Phys.* **123** (2020) 102470 [2006.02228].
- [16] M. Gottowik, C. Glaser, T. Huege and J. Rautenberg, *Astropart. Phys.* **103** (2018) 87 [1712.07442].
- [17] J.M. Alameddine et al., *Astropart. Phys.* **166** (2025) 103072 [2409.15999].
- [18] K. Bechtol et al., *Phys. Rev. D* **105** (2022) 063025 [2111.04334].

The Pierre Auger Collaboration



PIERRE
AUGER
OBSERVATORY

- A. Abdul Halim¹³, P. Abreu⁷⁰, M. Aglietta^{53,51}, I. Allekotte¹, K. Almeida Cheminant^{78,77}, A. Almela^{7,12}, R. Aloisio^{44,45}, J. Alvarez-Muñiz⁷⁶, A. Ambrosone⁴⁴, J. Ammerman Yebra⁷⁶, G.A. Anastasi^{57,46}, L. Anchordoqui⁸³, B. Andrade⁷, L. Andrade Dourado^{44,45}, S. Andringa⁷⁰, L. Apollonio^{58,48}, C. Aramo⁴⁹, E. Arnone^{62,51}, J.C. Arteaga Velázquez⁶⁶, P. Assis⁷⁰, G. Avila¹¹, E. Avocone^{56,45}, A. Bakalova³¹, F. Barbato^{44,45}, A. Bartz Mocellin⁸², J.A. Bellido¹³, C. Berat³⁵, M.E. Bertaina^{62,51}, M. Bianciotto^{62,51}, P.L. Biermann^a, V. Binet⁵, K. Bismarck^{38,7}, T. Bister^{77,78}, J. Biteau^{36,i}, J. Blazek³¹, J. Blümner⁴⁰, M. Boháčová³¹, D. Boncioli^{56,45}, C. Bonifazi⁸, L. Bonneau Arbeletche²², N. Borodai⁶⁸, J. Brack^f, P.G. Brichetto Orcher^{7,40}, F.L. Briechle⁴¹, A. Bueno⁷⁵, S. Buitink¹⁵, M. Buscemi^{46,57}, M. Büskens^{38,7}, A. Bwembya^{77,78}, K.S. Caballero-Mora⁶⁵, S. Cabana-Freire⁷⁶, L. Caccianiga^{58,48}, F. Campuzano⁶, J. Caraça-Valente⁸², R. Caruso^{57,46}, A. Castellina^{53,51}, F. Catalani¹⁹, G. Cataldi⁴⁷, L. Cazon⁷⁶, M. Cerda¹⁰, B. Čermáková⁴⁰, A. Cermenati^{44,45}, J.A. Chinellato²², J. Chudoba³¹, L. Chytha³², R.W. Clay¹³, A.C. Cobos Cerutti⁶, R. Colalillo^{59,49}, R. Conceição⁷⁰, G. Consolati^{48,54}, M. Conte^{55,47}, F. Convenga^{44,45}, D. Correia dos Santos²⁷, P.J. Costa⁷⁰, C.E. Covault⁸¹, M. Cristinziani⁴³, C.S. Cruz Sanchez³, S. Dasso^{4,2}, K. Daumiller⁴⁰, B.R. Dawson¹³, R.M. de Almeida²⁷, E.-T. de Boone⁴³, B. de Errico²⁷, J. de Jesús⁷, S.J. de Jong^{77,78}, J.R.T. de Mello Neto²⁷, I. De Mitri^{44,45}, J. de Oliveira¹⁸, D. de Oliveira Franco⁴², F. de Palma^{55,47}, V. de Souza²⁰, E. De Vito^{55,47}, A. Del Popolo^{57,46}, O. Deligny³³, N. Denner³¹, L. Deval^{53,51}, A. di Matteo⁵¹, C. Dobrigkeit²², J.C. D'Olivo⁶⁷, L.M. Domingues Mendes^{16,70}, Q. Dorost⁴³, J.C. dos Anjos¹⁶, R.C. dos Anjos²⁶, J. Ebr³¹, F. Ellwanger⁴⁰, R. Engel^{38,40}, I. Epicoco^{55,47}, M. Erdmann⁴¹, A. Etchegoyen^{7,12}, C. Evoli^{44,45}, H. Falcke^{77,79,78}, G. Farrar⁸⁵, A.C. Fauth²², T. Fehler⁴³, F. Feldbusch³⁹, A. Fernandes⁷⁰, M. Fernandez¹⁴, B. Fick⁸⁴, J.M. Figueira⁷, P. Filip^{38,7}, A. Filipčič^{74,73}, T. Fitoussi⁴⁰, B. Flagg⁸⁷, T. Fodran⁷⁷, A. Franco⁴⁷, M. Freitas⁷⁰, T. Fujii^{86,h}, A. Fuster^{7,12}, C. Galea⁷⁷, B. García⁶, C. Gaudí³⁷, P.L. Ghia³³, U. Giaccari⁴⁷, F. Gobbi¹⁰, F. Gollan⁷, G. Golup¹, M. Gómez Berisso¹, P.F. Gómez Vitale¹¹, J.P. Gongora¹¹, J.M. González¹, N. González⁷, D. Góra⁶⁸, A. Gorgi^{53,51}, M. Gottowik⁴⁰, F. Guarino^{59,49}, G.P. Guedes²³, L. Gültzow⁴⁰, S. Hahn³⁸, P. Hamal³¹, M.R. Hampel⁷, P. Hansen³, V.M. Harvey¹³, A. Haungs⁴⁰, T. Hebbeker⁴¹, C. Hojvat^d, J.R. Hörandel^{77,78}, P. Horvath³², M. Hrabovsky³², T. Huege^{40,15}, A. Insolia^{57,46}, P.G. Isar⁷², M. Ismaiel^{77,78}, P. Janecek³¹, V. Jilek³¹, K.-H. Kampert³⁷, B. Keilhauer⁴⁰, A. Khakurdi⁷⁷, V.V. Kizakke Covilakam^{7,40}, H.O. Klages⁴⁰, M. Kleifges³⁹, J. Köhler⁴⁰, F. Krieger⁴¹, M. Kubatova³¹, N. Kunka³⁹, B.L. Lago¹⁷, N. Langner⁴¹, N. Leal⁷, M.A. Leigui de Oliveira²⁵, Y. Lema-Capeans⁷⁶, A. Letessier-Selvon³⁴, I. Lhenry-Yvon³³, L. Lopes⁷⁰, J.P. Lundquist⁷³, M. Mallamaci^{60,46}, D. Mandat³¹, P. Mantsch^d, F.M. Mariani^{58,48}, A.G. Mariazzi³, I.C. Marić¹⁴, G. Marsella^{60,46}, D. Martello^{55,47}, S. Martinelli^{40,7}, M.A. Martins⁷⁶, H.-J. Mathes⁴⁰, J. Matthews^g, G. Matthiae^{61,50}, E. Mayotte⁸², S. Mayotte⁸², P.O. Mazur^d, G. Medina-Tanco⁶⁷, J. Meinert³⁷, D. Melo⁷, A. Menshikov³⁹, C. Merx⁴⁰, S. Michal³¹, M.I. Micheletti⁵, L. Miramonti^{58,48}, M. Mogarkar⁶⁸, S. Mollerach¹, F. Montanet³⁵, L. Morejon³⁷, K. Mulrey^{77,78}, R. Mussa⁵¹, W.M. Namasaka³⁷, S. Negi³¹, L. Nellen⁶⁷, K. Nguyen⁸⁴, G. Nicora⁹, M. Niechciol⁴³, D. Nitz⁸⁴, D. Nosek³⁰, A. Novikov⁸⁷, V. Novotny³⁰, L. Nožka³², A. Nucita^{55,47}, L.A. Núñez²⁹, J. Ochoa^{7,40}, C. Oliveira²⁰, L. Östman³¹, M. Palatka³¹, J. Pallotta⁹, S. Panja³¹, G. Parente⁷⁶, T. Paulsen³⁷, J. Pawlowsky³⁷, M. Pech³¹, J. Pěkala⁶⁸, R. Pelayo⁶⁴, V. Pelgrims¹⁴, L.A.S. Pereira²⁴, E.E. Pereira Martins^{38,7}, C. Pérez Bertolli^{7,40}, L. Perrone^{55,47}, S. Petrera^{44,45}, C. Petrucci⁵⁶, T. Pierog⁴⁰, M. Pimenta⁷⁰, M. Platino⁷, B. Pont⁷⁷, M. Pourmohammad Shahvar^{60,46}, P. Privitera⁸⁶, C. Priyatadarsi⁶⁸, M. Prouza³¹, K. Pytel⁶⁹, S. Querchfeld³⁷, J. Rautenberg³⁷, D. Ravignani⁷, J.V. Reginatto Akim²², A. Reuzki⁴¹, J. Ridky³¹, F. Riehn^{76,j}, M. Risse⁴³, V. Rizi^{56,45}, E. Rodriguez^{7,40}, G. Rodriguez Fernandez⁵⁰, J. Rodriguez Rojo¹¹, S. Rossoni⁴², M. Roth⁴⁰, E. Roulet¹, A.C. Rovero⁴, A. Saftoiu⁷¹, M. Saharan⁷⁷, F. Salamida^{56,45}, H. Salazar⁶³, G. Salina⁵⁰, P. Sampathkumar⁴⁰, N. San Martin⁸², J.D. Sanabria Gomez²⁹, F. Sánchez⁷, E.M. Santos²¹, E. Santos³¹, F. Sarazin⁸², R. Sarmento⁷⁰, R. Sato¹¹, P. Savina^{44,45}, V. Scherini^{55,47}, H. Schieler⁴⁰, M. Schimassek³³, M. Schimp³⁷, D. Schmidt⁴⁰, O. Scholten^{15,b}, H. Schoorlemmer^{77,78}, P. Schovánek³¹, F.G. Schröder^{87,40}, J. Schulte⁴¹, T. Schulz³¹, S.J. Sciutto³, M. Scornavacche⁷, A. Sedoski⁷, A. Segreto^{52,46}, S. Sehgal³⁷, S.U. Shivashankara⁷³, G. Sigl⁴², K. Simkova^{15,14}, F. Simon³⁹, R. Šmídá⁸⁶, P. Sommers^e, R. Squartini¹⁰, M. Stadelmaier^{40,48,58}, S. Stanić⁷³, J. Stasielak⁶⁸, P. Stassi³⁵, S. Strähn³⁸, M. Straub⁴¹, T. Suomijärvi³⁶, A.D. Supanitsky⁷, Z. Svozilikova³¹, K. Syrokvas³⁰, Z. Szadkowski⁶⁹, F. Tairli¹³, M. Tambone^{59,49}, A. Tapia²⁸, C. Taricco^{62,51}, C. Timmermans^{78,77}, O. Tkachenko³¹, P. Tobiska³¹, C.J. Todero Peixoto¹⁹, B. Tomé⁷⁰, A. Travaini¹⁰, P. Travnicek³¹, M. Tueros³, M. Unger⁴⁰, R. Uzeiroska³⁷, L. Vaclavek³², M. Vacula³², I. Vaiman^{44,45}, J.F. Valdés Galicia⁶⁷, L. Valore^{59,49}, P. van Dillen^{77,78}, E. Varela⁶³, V. Vašíčková³⁷, A. Vásquez-Ramírez²⁹, D. Veberič⁴⁰, I.D. Vergara Quispe³, S. Verpoest⁸⁷, V. Verzi⁵⁰, J. Vicha³¹, J. Vink⁸⁰, S. Vorobiov⁷³, J.B. Vuta³¹, C. Watanabe²⁷, A.A. Watson^c, A. Weindl⁴⁰, M. Weitz³⁷, L. Wiencke⁸², H. Wilczyński⁶⁸, B. Wundheiler⁷, B. Yue³⁷, A. Yushkov³¹, E. Zas⁷⁶, D. Zavrtanik^{73,74}, M. Zavrtanik^{74,73}

- ¹ Centro Atómico Bariloche and Instituto Balseiro (CNEA-UNCuyo-CONICET), San Carlos de Bariloche, Argentina
- ² Departamento de Física and Departamento de Ciencias de la Atmósfera y los Océanos, FCEyN, Universidad de Buenos Aires and CONICET, Buenos Aires, Argentina
- ³ IFLP, Universidad Nacional de La Plata and CONICET, La Plata, Argentina
- ⁴ Instituto de Astronomía y Física del Espacio (IAFE, CONICET-UBA), Buenos Aires, Argentina
- ⁵ Instituto de Física de Rosario (IFIR) – CONICET/U.N.R. and Facultad de Ciencias Bioquímicas y Farmacéuticas U.N.R., Rosario, Argentina
- ⁶ Instituto de Tecnologías en Detección y Astropartículas (CNEA, CONICET, UNSAM), and Universidad Tecnológica Nacional – Facultad Regional Mendoza (CONICET/CNEA), Mendoza, Argentina
- ⁷ Instituto de Tecnologías en Detección y Astropartículas (CNEA, CONICET, UNSAM), Buenos Aires, Argentina
- ⁸ International Center of Advanced Studies and Instituto de Ciencias Físicas, ECyT-UNSAM and CONICET, Campus Miguelete – San Martín, Buenos Aires, Argentina
- ⁹ Laboratorio Atmósfera – Departamento de Investigaciones en Láseres y sus Aplicaciones – UNIDEF (CITEDEF-CONICET), Argentina
- ¹⁰ Observatorio Pierre Auger, Malargüe, Argentina
- ¹¹ Observatorio Pierre Auger and Comisión Nacional de Energía Atómica, Malargüe, Argentina
- ¹² Universidad Tecnológica Nacional – Facultad Regional Buenos Aires, Buenos Aires, Argentina
- ¹³ University of Adelaide, Adelaide, S.A., Australia
- ¹⁴ Université Libre de Bruxelles (ULB), Brussels, Belgium
- ¹⁵ Vrije Universiteit Brussels, Brussels, Belgium
- ¹⁶ Centro Brasileiro de Pesquisas Fisicas, Rio de Janeiro, RJ, Brazil
- ¹⁷ Centro Federal de Educação Tecnológica Celso Suckow da Fonseca, Petropolis, Brazil
- ¹⁸ Instituto Federal de Educação, Ciência e Tecnologia do Rio de Janeiro (IFRJ), Brazil
- ¹⁹ Universidade de São Paulo, Escola de Engenharia de Lorena, Lorena, SP, Brazil
- ²⁰ Universidade de São Paulo, Instituto de Física de São Carlos, São Carlos, SP, Brazil
- ²¹ Universidade de São Paulo, Instituto de Física, São Paulo, SP, Brazil
- ²² Universidade Estadual de Campinas (UNICAMP), IFGW, Campinas, SP, Brazil
- ²³ Universidade Estadual de Feira de Santana, Feira de Santana, Brazil
- ²⁴ Universidade Federal de Campina Grande, Centro de Ciencias e Tecnologia, Campina Grande, Brazil
- ²⁵ Universidade Federal do ABC, Santo André, SP, Brazil
- ²⁶ Universidade Federal do Paraná, Setor Palotina, Palotina, Brazil
- ²⁷ Universidade Federal do Rio de Janeiro, Instituto de Física, Rio de Janeiro, RJ, Brazil
- ²⁸ Universidad de Medellín, Medellín, Colombia
- ²⁹ Universidad Industrial de Santander, Bucaramanga, Colombia
- ³⁰ Charles University, Faculty of Mathematics and Physics, Institute of Particle and Nuclear Physics, Prague, Czech Republic
- ³¹ Institute of Physics of the Czech Academy of Sciences, Prague, Czech Republic
- ³² Palacky University, Olomouc, Czech Republic
- ³³ CNRS/IN2P3, IJCLab, Université Paris-Saclay, Orsay, France
- ³⁴ Laboratoire de Physique Nucléaire et de Hautes Energies (LPNHE), Sorbonne Université, Université de Paris, CNRS-IN2P3, Paris, France
- ³⁵ Univ. Grenoble Alpes, CNRS, Grenoble Institute of Engineering Univ. Grenoble Alpes, LPSC-IN2P3, 38000 Grenoble, France
- ³⁶ Université Paris-Saclay, CNRS/IN2P3, IJCLab, Orsay, France
- ³⁷ Bergische Universität Wuppertal, Department of Physics, Wuppertal, Germany
- ³⁸ Karlsruhe Institute of Technology (KIT), Institute for Experimental Particle Physics, Karlsruhe, Germany
- ³⁹ Karlsruhe Institute of Technology (KIT), Institut für Prozessdatenverarbeitung und Elektronik, Karlsruhe, Germany
- ⁴⁰ Karlsruhe Institute of Technology (KIT), Institute for Astroparticle Physics, Karlsruhe, Germany
- ⁴¹ RWTH Aachen University, III. Physikalisches Institut A, Aachen, Germany
- ⁴² Universität Hamburg, II. Institut für Theoretische Physik, Hamburg, Germany
- ⁴³ Universität Siegen, Department Physik – Experimentelle Teilchenphysik, Siegen, Germany
- ⁴⁴ Gran Sasso Science Institute, L'Aquila, Italy
- ⁴⁵ INFN Laboratori Nazionali del Gran Sasso, Assergi (L'Aquila), Italy
- ⁴⁶ INFN, Sezione di Catania, Catania, Italy
- ⁴⁷ INFN, Sezione di Lecce, Lecce, Italy
- ⁴⁸ INFN, Sezione di Milano, Milano, Italy
- ⁴⁹ INFN, Sezione di Napoli, Napoli, Italy
- ⁵⁰ INFN, Sezione di Roma "Tor Vergata", Roma, Italy
- ⁵¹ INFN, Sezione di Torino, Torino, Italy

- ⁵² Istituto di Astrofisica Spaziale e Fisica Cosmica di Palermo (INAF), Palermo, Italy
⁵³ Osservatorio Astrofisico di Torino (INAF), Torino, Italy
⁵⁴ Politecnico di Milano, Dipartimento di Scienze e Tecnologie Aerospaziali , Milano, Italy
⁵⁵ Università del Salento, Dipartimento di Matematica e Fisica “E. De Giorgi”, Lecce, Italy
⁵⁶ Università dell’Aquila, Dipartimento di Scienze Fisiche e Chimiche, L’Aquila, Italy
⁵⁷ Università di Catania, Dipartimento di Fisica e Astronomia “Ettore Majorana“, Catania, Italy
⁵⁸ Università di Milano, Dipartimento di Fisica, Milano, Italy
⁵⁹ Università di Napoli “Federico II”, Dipartimento di Fisica “Ettore Pancini”, Napoli, Italy
⁶⁰ Università di Palermo, Dipartimento di Fisica e Chimica ”E. Segrè”, Palermo, Italy
⁶¹ Università di Roma “Tor Vergata”, Dipartimento di Fisica, Roma, Italy
⁶² Università Torino, Dipartimento di Fisica, Torino, Italy
⁶³ Benemérita Universidad Autónoma de Puebla, Puebla, México
⁶⁴ Unidad Profesional Interdisciplinaria en Ingeniería y Tecnologías Avanzadas del Instituto Politécnico Nacional (UPIITA-IPN), México, D.F., México
⁶⁵ Universidad Autónoma de Chiapas, Tuxtla Gutiérrez, Chiapas, México
⁶⁶ Universidad Michoacana de San Nicolás de Hidalgo, Morelia, Michoacán, México
⁶⁷ Universidad Nacional Autónoma de México, México, D.F., México
⁶⁸ Institute of Nuclear Physics PAN, Krakow, Poland
⁶⁹ University of Łódź, Faculty of High-Energy Astrophysics, Łódź, Poland
⁷⁰ Laboratório de Instrumentação e Física Experimental de Partículas – LIP and Instituto Superior Técnico – IST, Universidade de Lisboa – UL, Lisboa, Portugal
⁷¹ “Horia Hulubei” National Institute for Physics and Nuclear Engineering, Bucharest-Magurele, Romania
⁷² Institute of Space Science, Bucharest-Magurele, Romania
⁷³ Center for Astrophysics and Cosmology (CAC), University of Nova Gorica, Nova Gorica, Slovenia
⁷⁴ Experimental Particle Physics Department, J. Stefan Institute, Ljubljana, Slovenia
⁷⁵ Universidad de Granada and C.A.F.P.E., Granada, Spain
⁷⁶ Instituto Galego de Física de Altas Enerxías (IGFAE), Universidade de Santiago de Compostela, Santiago de Compostela, Spain
⁷⁷ IMAPP, Radboud University Nijmegen, Nijmegen, The Netherlands
⁷⁸ Nationaal Instituut voor Kernfysica en Hoge Energie Fysica (NIKHEF), Science Park, Amsterdam, The Netherlands
⁷⁹ Stichting Astronomisch Onderzoek in Nederland (ASTRON), Dwingeloo, The Netherlands
⁸⁰ Universiteit van Amsterdam, Faculty of Science, Amsterdam, The Netherlands
⁸¹ Case Western Reserve University, Cleveland, OH, USA
⁸² Colorado School of Mines, Golden, CO, USA
⁸³ Department of Physics and Astronomy, Lehman College, City University of New York, Bronx, NY, USA
⁸⁴ Michigan Technological University, Houghton, MI, USA
⁸⁵ New York University, New York, NY, USA
⁸⁶ University of Chicago, Enrico Fermi Institute, Chicago, IL, USA
⁸⁷ University of Delaware, Department of Physics and Astronomy, Bartol Research Institute, Newark, DE, USA

^a Max-Planck-Institut für Radioastronomie, Bonn, Germany^b also at Kapteyn Institute, University of Groningen, Groningen, The Netherlands^c School of Physics and Astronomy, University of Leeds, Leeds, United Kingdom^d Fermi National Accelerator Laboratory, Fermilab, Batavia, IL, USA^e Pennsylvania State University, University Park, PA, USA^f Colorado State University, Fort Collins, CO, USA^g Louisiana State University, Baton Rouge, LA, USA^h now at Graduate School of Science, Osaka Metropolitan University, Osaka, Japanⁱ Institut universitaire de France (IUF), France^j now at Technische Universität Dortmund and Ruhr-Universität Bochum, Dortmund and Bochum, Germany

Acknowledgments

The successful installation, commissioning, and operation of the Pierre Auger Observatory would not have been possible without the strong commitment and effort from the technical and administrative staff in Malargüe. We are very grateful to the following agencies and organizations for financial support:

Argentina – Comisión Nacional de Energía Atómica; Agencia Nacional de Promoción Científica y Tecnológica (ANPCyT); Consejo Nacional de Investigaciones Científicas y Técnicas (CONICET); Gobierno de la Provincia de

Mendoza; Municipalidad de Malargüe; NDM Holdings and Valle Las Leñas; in gratitude for their continuing cooperation over land access; Australia – the Australian Research Council; Belgium – Fonds de la Recherche Scientifique (FNRS); Research Foundation Flanders (FWO), Marie Curie Action of the European Union Grant No. 101107047; Brazil – Conselho Nacional de Desenvolvimento Científico e Tecnológico (CNPq); Financiadora de Estudos e Projetos (FINEP); Fundação de Amparo à Pesquisa do Estado de Rio de Janeiro (FAPERJ); São Paulo Research Foundation (FAPESP) Grants No. 2019/10151-2, No. 2010/07359-6 and No. 1999/05404-3; Ministério da Ciência, Tecnologia, Inovações e Comunicações (MCTIC); Czech Republic – GACR 24-13049S, CAS LQ100102401, MEYS LM2023032, CZ.02.1.01/0.0/0.0/16_013/0001402, CZ.02.1.01/0.0/0.0/18_046/0016010 and CZ.02.1.01/0.0/0.0/17_049/0008422 and CZ.02.01.01/00/22_008/0004632; France – Centre de Calcul IN2P3/CNRS; Centre National de la Recherche Scientifique (CNRS); Conseil Régional Ile-de-France; Département Physique Nucléaire et Corpusculaire (PNC-IN2P3/CNRS); Département Sciences de l'Univers (SDU-INSU/CNRS); Institut Lagrange de Paris (ILP) Grant No. LABEX ANR-10-LABX-63 within the Investissements d'Avenir Programme Grant No. ANR-11-IDEX-0004-02; Germany – Bundesministerium für Bildung und Forschung (BMBF); Deutsche Forschungsgemeinschaft (DFG); Finanzministerium Baden-Württemberg; Helmholtz Alliance for Astroparticle Physics (HAP); Helmholtz-Gemeinschaft Deutscher Forschungszentren (HGF); Ministerium für Kultur und Wissenschaft des Landes Nordrhein-Westfalen; Ministerium für Wissenschaft, Forschung und Kunst des Landes Baden-Württemberg; Italy – Istituto Nazionale di Fisica Nucleare (INFN); Istituto Nazionale di Astrofisica (INAF); Ministero dell'Università e della Ricerca (MUR); CETEMPS Center of Excellence; Ministero degli Affari Esteri (MAE), ICSC Centro Nazionale di Ricerca in High Performance Computing, Big Data and Quantum Computing, funded by European Union NextGenerationEU, reference code CN_00000013; México – Consejo Nacional de Ciencia y Tecnología (CONACYT) No. 167733; Universidad Nacional Autónoma de México (UNAM); PAPIIT DGAPA-UNAM; The Netherlands – Ministry of Education, Culture and Science; Netherlands Organisation for Scientific Research (NWO); Dutch national e-infrastructure with the support of SURF Cooperative; Poland – Ministry of Education and Science, grants No. DIR/WK/2018/11 and 2022/WK/12; National Science Centre, grants No. 2016/22/M/ST9/00198, 2016/23/B/ST9/01635, 2020/39/B/ST9/01398, and 2022/45/B/ST9/02163; Portugal – Portuguese national funds and FEDER funds within Programa Operacional Factores de Competitividade through Fundação para a Ciência e a Tecnologia (COMPETE); Romania – Ministry of Research, Innovation and Digitization, CNCS-UEFISCDI, contract no. 30N/2023 under Romanian National Core Program LAPLAS VII, grant no. PN 23 21 01 02 and project number PN-III-P1-1.1-TE-2021-0924/TE57/2022, within PNCDI III; Slovenia – Slovenian Research Agency, grants P1-0031, P1-0385, I0-0033, N1-0111; Spain – Ministerio de Ciencia e Innovación/Agencia Estatal de Investigación (PID2019-105544GB-I00, PID2022-140510NB-I00 and RYC2019-027017-I), Xunta de Galicia (CIGUS Network of Research Centers, Consolidación 2021 GRC GI-2033, ED431C-2021/22 and ED431F-2022/15), Junta de Andalucía (SOMM17/6104/UGR and P18-FR-4314), and the European Union (Marie Skłodowska-Curie 101065027 and ERDF); USA – Department of Energy, Contracts No. DE-AC02-07CH11359, No. DE-FR02-04ER41300, No. DE-FG02-99ER41107 and No. DE-SC0011689; National Science Foundation, Grant No. 0450696, and NSF-2013199; The Grainger Foundation; Marie Curie-IRSES/EPLANET; European Particle Physics Latin American Network; and UNESCO. The authors gratefully acknowledge the computing time provided on the high-performance computer HoreKa by the National High-Performance Computing Center at KIT (NHR@KIT). This center is jointly supported by the Federal Ministry of Education and Research and the Ministry of Science, Research and the Arts of Baden-Württemberg, as part of the National High-Performance Computing (NHR) joint funding program. HoreKa is partly funded by the German Research Foundation.